Thermodynamic determination of low melting area in $CaO-Al_2O_3-SiO_2-MgO-MnO$ system inclusion and its control in spring steel

Bo ZHANG[1),2)], Fuming WANG[1),2)] and Changrong LI[3)]

1) School of Metallurgical and Ecological Engineering, University of Science and Technology Beijing, 100083, China

2) State Key Laboratory of Advanced Metallurgy, University of Science and Technology Beijing, 100083, China

3) School of Material Science and Engineering, University of Science and Technology Beijing, 100083, China

Abstract: Considering the importance of $CaO-Al_2O_3-SiO_2-MgO-MnO$ system in spring steel production, the present authors calculated 1000 liquidus projection figures of this system with CALPHAD technique. The effect of each oxide component on low melting point area (below 1673K) of this system has been attained. Furthermore, the system with the maximum low melting point area, i.e., CaO-19.23%Al_2O_3-SiO_2-3.85%MgO-MnO, has been obtained. On the basis of the previous work, the contents of solutes: oxygen, aluminum, calcium, and magnesium in liquid steel of many spring grades have been computed by using FactSage software under condition of the inclusion compositions in the steel falling in the low melting point area of CaO-19.23%Al_2O_3-SiO_2-3.85%MgO-MnO system. In addition, the controlled ranges of the low point inclusion composition and those of the liquid steel in equilibrium with the inclusion were determined on the condition of very low dissolved oxygen contents. As an example, the calculated results for 60Si2Cr grade steel refining are exhibited in the present paper.

Keywords: $CaO-Al_2O_3-SiO_2-MgO-MnO$ system, inclusion, low melting point zone, thermodynamics

1. Introduction

The effect of inclusion on fatigue property of spring steels is generally very great. With the development of high-stress spring steel, the influence of non-metallic inclusions on fatigue strength of springs in steels will become more noticeable. In order to reduce the harmful effect of high melting point and undeformable Al_2O_3-rich inclusions such as Al_2O_3, $CaO\cdot Al_2O_3$ and $MgO\cdot Al_2O_3$ on fatigue strength of valve springs, Si/Mn deoxidation is mostly used in the production of spring steel wires, special synthetic flux is made to modify Al_2O_3-rich oxide inclusions, which generates low melting point and good deformability inclusion with $CaO-Al_2O_3-SiO_2-MnO$ system. However, the inclusions formed usually contain a certain amount of MgO due to the effect of MgO in refractory lines or slag in the melting process, which resulted in the inclusions belonging to $CaO-Al_2O_3-SiO_2-MgO-MnO$ system. The experimental results by Chai Guoqiang[1] et al showed that nearly fifty percent inclusions belong to $CaO-Al_2O_3-SiO_2-MgO-MnO$ system in 82B high-carbon hard wire steel. In previous studies, the composition controls of $CaO-Al_2O_3-SiO_2$, $Al_2O_3-SiO_2-MnO$, $CaO-Al_2O_3-SiO_2-MnO$ and $CaO-Al_2O_3-SiO_2-MgO$ inclusions have been reported [2-6], but the composition control of $CaO-Al_2O_3-SiO_2-MgO-MnO$ system inclusion has been not studied.

In this paper, the projection figures of liquidus of inclusions with $CaO-Al_2O_3-SiO_2-MgO-MnO$ system have been calculated based on FactSage thermodynamic software, the effect rule of each component on low melting point area of this system was analyzed and discussed, and the control ranges of composition of $CaO-Al_2O_3-SiO_2-MgO-MnO$ inclusion with largest low melting point area were given. Then, the composition of liquid steel when these inclusions

mentioned above form in 60Si2Cr valve spring steel at 1873K was computed.

2. Methods of calculation and thermodynamic data

The liquidus projection figures of inclusions with CaO-Al_2O_3-SiO_2-MgO-MnO system and all its ternary and quaternary subsystem and databases of component composition and activity of this system were calculated on the basis of Phase Diagram and Equilib module from FactSage thermodynamic software, respectively. FToxid Oxide database of this software was used when computing. Gibbs Free Energy of the molten oxide phase in the database was computed by the Modified Quasi-chemical Model[8, 9]. This database has been evaluated and optimized. Thus, all computation results of this work are accurate and believable.

The average composition of 60Si2Cr spring steel was chosen, not taking into account impurity element contents, namely, [C%]=0.6, [Si%]=1.6, [Mn%]=0.55, [Cr%]=0.85 (weight percentage) when the control on low melting point CaO-Al_2O_3-SiO_2-MgO-MnO system inclusions for 60Si2Cr liquid spring steel was calculated thermodynamically. The activities of various solutes in this liquid steel and activity coefficients were computed by Eqs. (1) and (2), respectively. This reference state is designated as 1 mass % solution. The first-order interaction coefficients (e_i^j) related with activity coefficients and the chemical reactions occurring between hot steel and inclusions and their Gibbs Free Energy are given in Tables 1[4, 10-11] and 2[12, 13], respectively.

$$a_i = f_i \cdot [\%i] \qquad \text{(Eq. 1)}$$

$$\lg f_i = \sum_j e_i^j \cdot [\%j] + \sum_{j,k} r_i^{j,k} \cdot [\%j] \cdot [\%k] \qquad \text{(Eq. 2)}$$

Table 1 First-order interaction coefficients (e_i^j) at 1873K used in this work

	j							
i	Al	C	O	Mn	Si	Cr	Mg	Ca
Al	0.045	0.091	-6.6	0.0065	0.056	0.012	-0.13	-0.047
O	-3.9	-0.0436	-0.2	-0.021	-0.131	-0.0459	-190	-3600
Mn	-	-0.07	-0.083	0	0	0.0039	-	-0.023
Si	0.058	0.18	-0.23	0.002	0.11	-0.0003	-	-0.067
Ca	-0.072	-0.34	-9000	-0.0156	-0.097	0.02	-	-0.002
Mg	-0.12	-0.24	-289	-	-0.09	0.05	-	-

Table 2 Chemical reactions occurring between molten steel and inclusion and their Gibbs Free Energies

Number	chemical reaction equations	ΔG^o (J/mol)
1	$[Si]+2[O]=(SiO_2)$	-581900+221.8T
2	$2/3(Al_2O_3)+[Si]=(SiO_2)+4/3[Al]$	219400-35.7T
3	$2[Ca]+(SiO_2)=2(CaO)+[Si]$	-694422+75.06T
4	$2[Mg]+(SiO_2)=2(MgO)+[Si]$	-875300+255T

3. Optimizations of low melting point zone of CaO-Al_2O_3-SiO_2-MgO-MnO system inclusions

The relationship between deformability of inclusion and temperature was studied by G. Bernard[2] and it was indicated that with respect to CaO-Al_2O_3-SiO_2 system inclusions, if their compositions are near anorthite ($CaO \cdot Al_2O_3 \cdot SiO_2$) and tridymite ($SiO_2$) and wollastonite ($CaO \cdot SiO_2$), they have good deformability, the melting point of inclusions in this low melting point zone is lower than 1400℃. In this article, the region with lower than 1400℃

melting point of inclusions of CaO-Al_2O_3-SiO_2-MgO-MnO system is defined as the low melting point zone, and it is considered that the inclusions in this low melting point zone have good deformability. In this section, the effect rule of each component on low melting point zone size of CaO-Al_2O_3-SiO_2-MgO-MnO system was analyzed systematically, the compositions range of inclusions was given when low melting point zone was the largest. The liquidus projection figures of 1000 inclusions with CaO-Al_2O_3-SiO_2-MgO-MnO system were calculated based on FactSage thermodynamic software. The design principle of composition of 1000 inclusions with CaO-Al_2O_3-SiO_2-MgO-MnO system is as follows: two components of five components including CaO, Al_2O_3, SiO_2, MgO and MnO was chosen randomly (amounting to 10 groups), and the weight ratio of the selected two components and the residual three components was in turn fixed as 0, 0.05, 0.1, 0.15, 0.20, 0.25, 0.30, 0.35, 0.40 and 0.45. Then, permutation and combination were done, which obtained 100 systems (P_{10}^{10} =100). Ten groups amount to 1000 systems.

The low melting point zone sizes of CaO-Al_2O_3-SiO_2-MgO-MnO system varying with different contents of MnO and MgO, MgO and CaO, CaO and MnO, SiO_2 and CaO, Al_2O_3 and CaO, Al_2O_3 and MgO, MgO and SiO_2, SiO_2 and Al_2O_3, MnO and SiO_2 and MnO and Al_2O_3 are showed in Fig.1(a)～(j). The change rules can be seen from above figures about the low melting point zone size of the systems. Here only analysis was conducted on particularly Figure 1(a) and 1(b). It is indicated in Figure 1(a) that the low melting point zone size of the system increases basically with addition of MnO content when MgO content is varied. When MnO content is different, the low melting point zone size of the system first increases with addition of MgO content and then decreases. When MgO content and MnO content is 0.05 and 0.35, respectively, the low melting point zone size of the system is the largest, viz. about 45%. Figure 1(b) indicated that the low melting point zone size of the system increases first with addition of MgO content and then decreases when CaO content is varied. When CaO content is 0.45, and MgO content is 0.05 or 0.1, the low melting point zone size of the system is the largest, viz. approximately 51%.

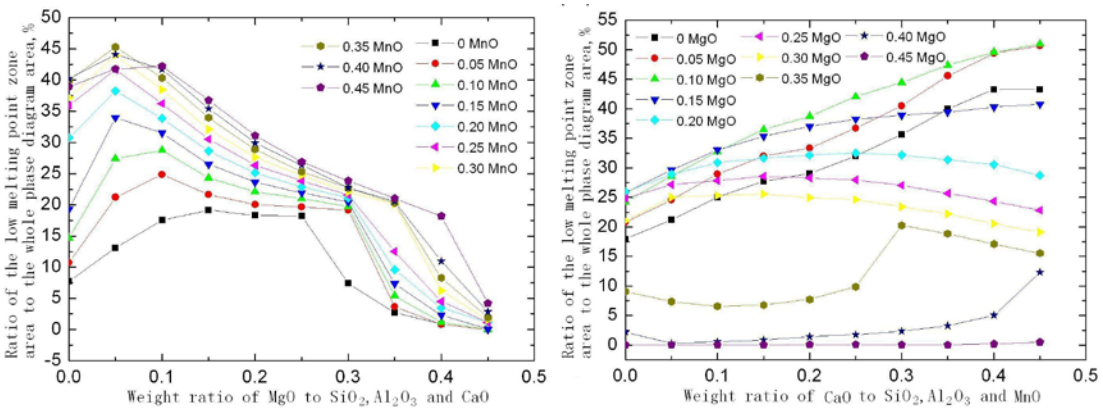

(a) (b)

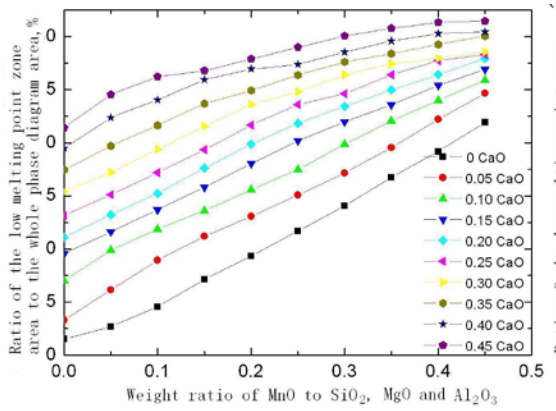
Ratio of the low melting point zone area to the whole phase diagram area, %
Weight ratio of MnO to SiO_2, MgO and Al_2O_3
0 CaO
0.05 CaO
0.10 CaO
0.15 CaO
0.20 CaO
0.25 CaO
0.30 CaO
0.35 CaO
0.40 CaO
0.45 CaO

(c)

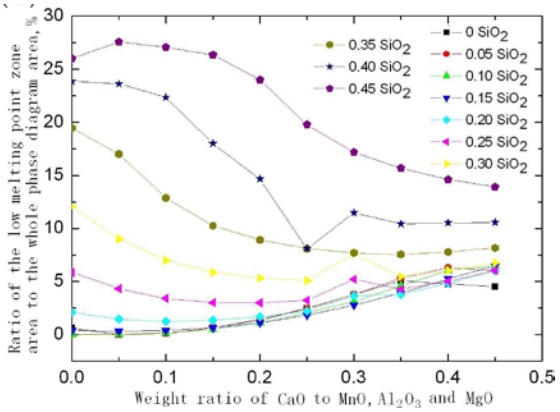
Ratio of the low melting point zone area to the whole phase diagram area, %
Weight ratio of CaO to MnO, Al_2O_3 and MgO
0 SiO_2
0.05 SiO_2
0.10 SiO_2
0.15 SiO_2
0.20 SiO_2
0.25 SiO_2
0.30 SiO_2
0.35 SiO_2
0.40 SiO_2
0.45 SiO_2

(d)

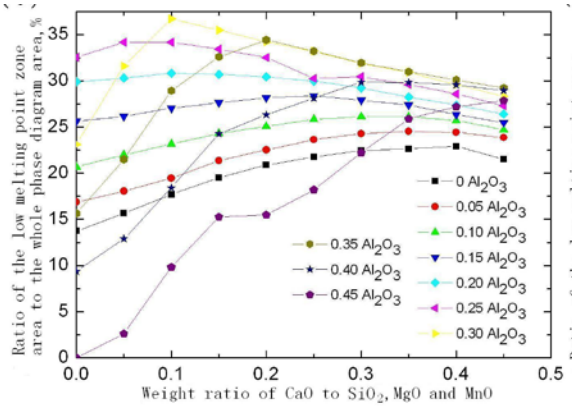
Ratio of the low melting point zone area to the whole phase diagram area, %
Weight ratio of CaO to SiO_2, MgO and MnO
0 Al_2O_3
0.05 Al_2O_3
0.10 Al_2O_3
0.15 Al_2O_3
0.20 Al_2O_3
0.25 Al_2O_3
0.30 Al_2O_3
0.35 Al_2O_3
0.40 Al_2O_3
0.45 Al_2O_3

(e)

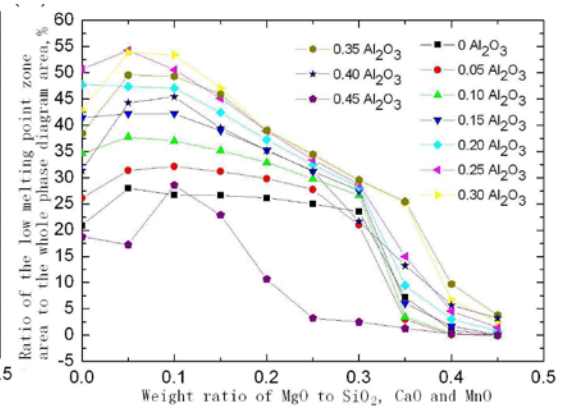
Ratio of the low melting point zone area to the whole phase diagram area, %
Weight ratio of MgO to SiO_2, CaO and MnO
0 Al_2O_3
0.05 Al_2O_3
0.10 Al_2O_3
0.15 Al_2O_3
0.20 Al_2O_3
0.25 Al_2O_3
0.30 Al_2O_3
0.35 Al_2O_3
0.40 Al_2O_3
0.45 Al_2O_3

(f)

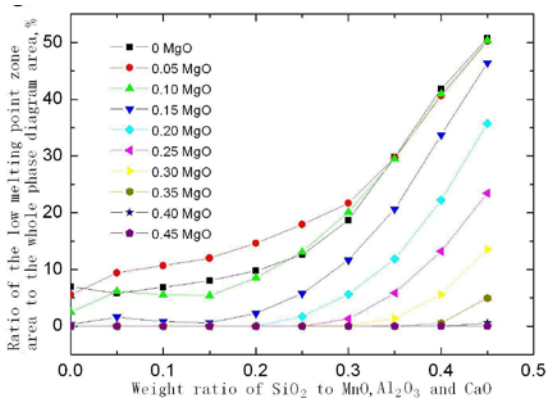
Ratio of the low melting point zone area to the whole phase diagram area, %
Weight ratio of SiO_2 to MnO, Al_2O_3 and CaO
0 MgO
0.05 MgO
0.10 MgO
0.15 MgO
0.20 MgO
0.25 MgO
0.30 MgO
0.35 MgO
0.40 MgO
0.45 MgO

(g)

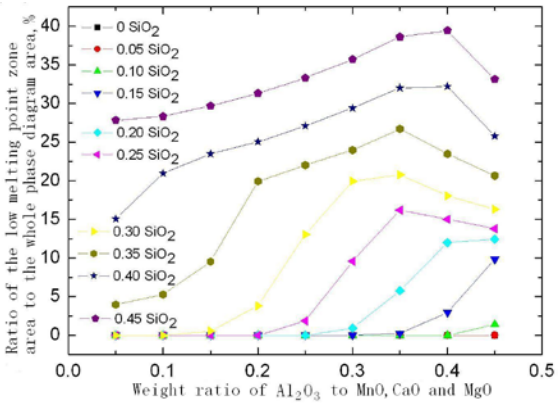
Ratio of the low melting point zone area to the whole phase diagram area, %
Weight ratio of Al_2O_3 to MnO, CaO and MgO
0 SiO_2
0.05 SiO_2
0.10 SiO_2
0.15 SiO_2
0.20 SiO_2
0.25 SiO_2
0.30 SiO_2
0.35 SiO_2
0.40 SiO_2
0.45 SiO_2

(h)

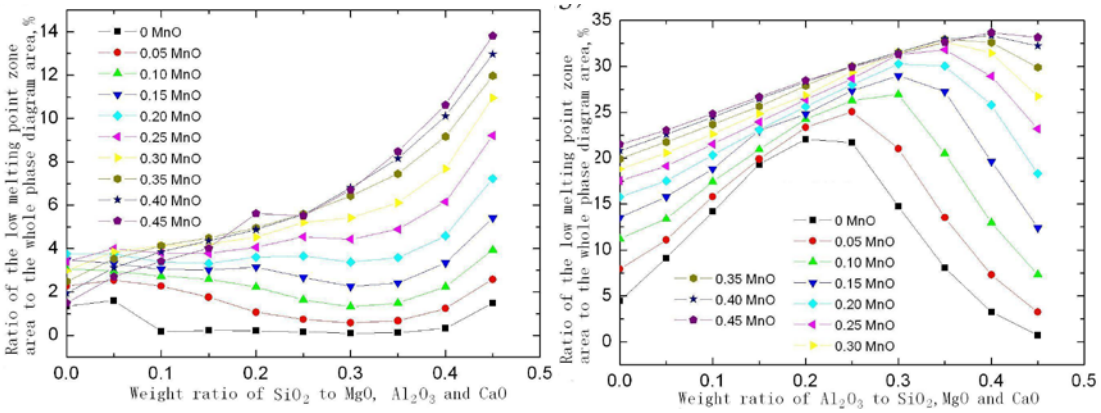

(i) (j)

Fig. 1 Change in area percentage of the low melting point zone with different two component contents in $CaO-Al_2O_3-SiO_2-MgO-MnO$ system. (a) MnO and MgO; (b) MgO and CaO; (c) CaO and MnO; (d) SiO_2 and CaO; (e) Al_2O_3 and CaO; (f) Al_2O_3 and MgO; (g) MgO and SiO_2; (h) SiO_2 and Al_2O_3; (i) MnO and SiO_2; (j) MnO and Al_2O_3

The low melting point zone is larger, the low melting point control of inclusions is easier. Therefore, in order to obtain the composition ranges of inclusions with the maximum low melting point zone of $CaO-Al_2O_3-SiO_2-MgO-MnO$ systems, the low melting point zone sizes of 1000 $CaO-Al_2O_3-SiO_2-MgO-MnO$ systems from Figure 1(a)～(j) were compared. It is found that the low melting point zone size of some systems from Figure 1(b), Figure 1(f) and Figure 1(g) are larger, percentage ratio of area of low melting point zone to area of the whole phase diagram is about 50%. All these systems were given in Table 3. Table 3 shows that MgO content of 14 systems in Table 3 is very low and varies from 0 to 8%. The area of the low melting point zone of ninth system in Table 3 is the largest.

Table 3 Composition for $CaO-Al_2O_3-SiO_2-MgO-MnO$ systems when the area percentage of low melting point zone is about 50%

Number	The total weight ratio of selected two components and residual three components	The percentage of area of low melting point zone accounting for area of the whole phase diagram /%	composition*/%				
			MgO	CaO	Al_2O_3	SiO_2	MnO
1	MgO=0，SiO_2=0.45	50.7	0	0～61	0～52	31.03	0～95
2	MgO=0.05，SiO_2=0.45	50.2	3.33	0～65	0～43	30	0～90
3	MgO=0.10，SiO_2=0.45	50.4	6.45	0～70	0～43	29.03	0～95
4	MgO=0.05，CaO=0.40	49.4	3.45	27.59	0～71	0～92	0～57
5	MgO=0.10，CaO =0.40	49.6	6.67	24.67	0～82	0～95	0～55
6	MgO=0.05，CaO=0.45	50.7	3.33	30	0～75	0～95	0～55
7	MgO=0.10，CaO =0.45	50.9	6.45	29.03	0～85	0～98	0～53
8	MgO=0，Al_2O_3=0.25	50.7	0	0～62	20	16～88	0～78
9	MgO=0.05，Al_2O_3=0.25	54.3	3.85	0～63	19.23	18～90	0～80
10	MgO=0.05，Al_2O_3=0.30	53.9	3.70	0～70	22.22	15～92	0～72
11	MgO=0.05，Al_2O_3=0.35	49.6	3.57	0～74	25	12～92	0～65

12	MgO=0.10，Al_2O_3=0.25	50.6	7.41	0～48	18.52	22～90	0～60
13	MgO=0.10，Al_2O_3=0.30	53.4	7.14	0～66	21.43	20～92	0～80
14	MgO=0.10，Al_2O_3=0.35	49.3	6.90	0～70	24.14	18～90	0～75

Note *：The selected two components have been converted into weight percent, the sum of weight percent of residual three components is 100%.

4. Composition of liquid steel when low melting point inclusions with the system forming in spring steel

It is found from Table 3 that CaO-19.23%Al_2O_3-SiO_2-3.85%MgO-MnO system has the largest low melting point zone. Thus, 60Si2Cr valve spring steel is taken as an example in this section, [Al] content, [Ca] content, [Mg] content and [O] content have been computed when inclusion compositions in molten steel are located in low melting point zone of CaO-19.23%Al_2O_3-SiO_2-3.85%MgO-MnO system.

Figure 2(a), (b), (c) and (d) are, respectively, iso-[O] lines, iso-[Al] lines, iso-[Ca] activity lines and iso-[Mg] activity lines calculated according to chemical reaction eqs.1, 2, 3 and 4 in Table 2. It is found from Figure 2 that the ranges of [O] content, [Al] content, [Ca] activity and [Mg] activity are 2～80 ppm, 2～280 ppm, 0～1.5×10^{-7} and 0～3×10^{-5}, respectively, when the low melting point inclusions of CaO-19.23%Al_2O_3-SiO_2-3.85%MgO-MnO system forming in molten 60Si2Cr spring steel. Considering that the dissolved [O] content of spring steel product can not be too high, accordingly, optimal inclusion composition is SiO_2=20～40%, MnO=10～70%, CaO=10～60% (wt%), viz. this region surrounded by iso-[O] line of 10 ppm in Figure 2(a) and liqudus of 1400℃. Under this condition, the dissolved [O] content of molten steel was 2～10 ppm, the dissolved [Al] content was 30～280 ppm, [Ca] activity was 5.0×10^{-10}～1.5×10^{-7} and [Mg] activity was 1.0×10^{-6}～3.0×10^{-5}. The contradiction between the required low dissolved [O] content of liquid steel and the plastification of inclusion can be solved through controlling formation of inclusion located in the low melting point zone of CaO-19.23%Al_2O_3-SiO_2-3.85%MgO-MnO system mentioned above, and which is not so strict with the requirement of dissolved [Al] content in liquid steel.

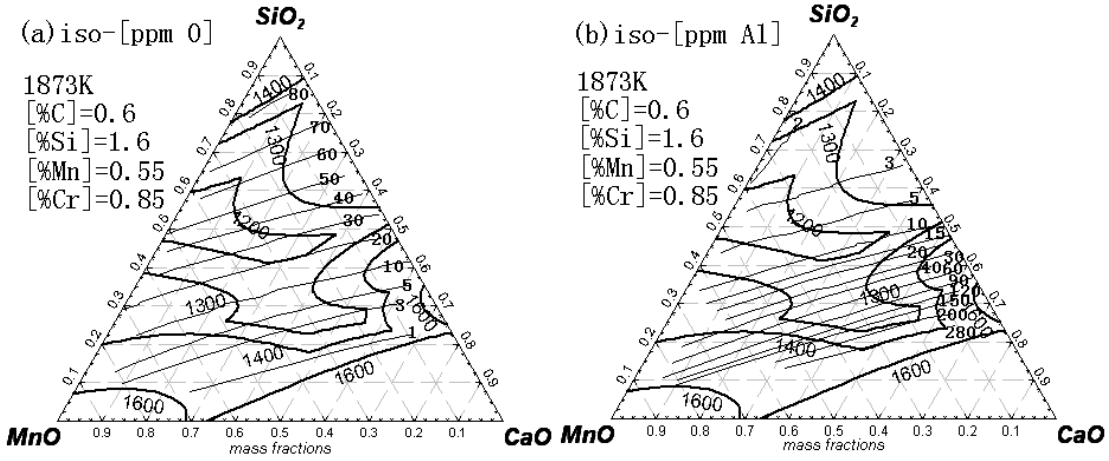

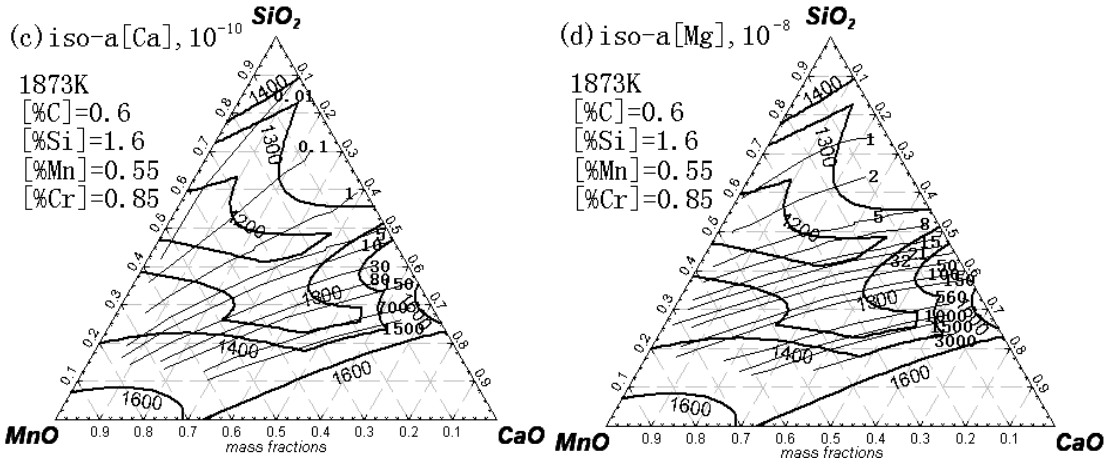

Fig. 2 Iso-[O], iso-[Al], iso-a[Ca] and iso-a[Ca] lines on the equilibrium established between molten 60Si2Cr spring steel and CaO-19.23%Al_2O_3-SiO_2-3.85%MgO-MnO inclusions

5. Conclusions

The effect rule of each component on the low melting point zone size of the system studied has been given through calculation and analysis of liquidus projection figures of 1000 in CaO-Al_2O_3-SiO_2-MgO-MnO system and ternary and quaternary subsystems of the quinary system. CALPHAD technique has been used along with software FactSage in the calculation. Furthermore, the system with the maximum low melting point zone has been found by comparing, viz. CaO-19.23%Al_2O_3-SiO_2-3.85%MgO-MnO system. The optimal inclusion composition is SiO_2=20～40%, MnO=10～70%, CaO=10～60% when composition of inclusion forming in liquid 60Si2Cr spring steel at 1873 K is located in the low melting point area of CaO-19.23%Al_2O_3-SiO_2-3.85%MgO-MnO system on condition that the dissolved [O] content be lower. Under this condition, the dissolved [O] content, the dissolved [Al] content, the dissolved [Ca] activity, the dissolved [Mg] activity of the liquid steel was 2～10 ppm, 30～280 ppm, 5.0×10^{-10}～1.5×10^{-7} and 1.0×10^{-6}～3.0×10^{-5}, respectively.

Acknowledgment

The authors would like to be grateful for the National Natural Science Fund (50874007) for their financial support.

References

[1] G. Q. Chai, F. M. Wang, J. Fu, C. R. Li. Deformability control of Al_2O_3-SiO_2-MgO-CaO-MnO system inclusions in high carbon hard wire 82B steel. *Journal of University of Science and Technology Beijing*, 2010, 32(6), p 730–734, in Chinese.

[2] G. Bernard, P. V. Ribord, G. Urbain. Oxide inclusions plasticity. *Revue de Metallurgie-CIT*, 1981, 78(5), p 421–423.

[3] S. Maeda, T. Soejima. Shape control of inclusions in wire rods for high tensile tire cord by refining with synthetic slag. *Steelmaking Conference Proceedings*, 1989, p 379–385.

[4] S. Hideaki, I. Ryo. Thermodynamics on control of inclusion composition in ultra clean steels. *ISIJ Int.* , 1996, 36(5), p 528–536.

[5] L. L. Jin, H. T. Wang, Z. B. Xu, F. M. Wang. Control on low melting point area in a CaO-SiO_2-Al_2O_3-MnO system.

Journal of University of Science and Technology Beijing, 2007, 29(6), p 576, in Chinese.

[6] H. T. Wang, F. M. Wang, Z. B. Xu, L. L. Jin. Composition control of CaO-MgO-Al_2O_3-SiO_2 inclusions in tire cord steel-a thermodynamic analysis. *Steel research international*, 2008, 79(1), p 25–30, in Chinese.

[7] C. W. Bale, P. Chartrand, S. A. Decterov, K. Hack, R. B. Mahfoud, J. Melancon, A. D. Pelon, S. Petersen. FactSage thermochemical software and databases. *CALPHAD*, 2002, 26(2), p 189–228.

[8] A. D. Pelton, M. Blander. Thermodynamic analysis of ordered liquid solutions by a modified quasichemical approach-application to silicate slags. *Metall. Trans. B*, 1986, 17B, p 805.

[9] A. D. Pelton, S. A. Decterov, G. Eriksson. The modified quasichemical model ~~—~~binary solutions. *Metall. Mater. Trans. B*, 2000, 31B(8), p 651.

[10] G. K. Sigworth, J. F. Elliott. The thermodynamics of liquid dilute iron alloys. *Met. Sci.* , 1974, 18, p 298–310.

[11] M. Kishi, R. Inoue, H. Suito. Thermodynamics of oxygen and nitrogen in liquid Fe-20 mass%Cr alloy equilibrated with Titania-based slags. *ISIJ Int.* , 1994, 34(11), p 859.

[12] H. Ohta, H. Suito. Activities in MnO-SiO_2-Al_2O_3 slags and deoxidation equilibria of Mn and Si. *Metallurgical and Materials Transactions B*, 1996, 27B(4), p 263–270.

[13] H. Ohta, H. Suito. Activities in CaO-MgO-Al_2O_3 slags and deoxidation equilibria of Al, Mg and Ca. *ISIJ International*, 1996, 36(8), p 983–990.